Valproic acid prevents glucocorticoid-induced osteonecrosis of the femoral head of rats

DING ZHOU[1], YI-XUAN CHEN[1], JUN-HUI YIN[2], SHI-CONG TAO[1], SHANG-CHUN GUO[2], ZHAN-YING WEI[3], YONG FENG[1] and CHANG-QING ZHANG[1]

[1]Department of Orthopaedic Surgery, Shanghai Jiao Tong University Affiliated Sixth People's Hospital; [2]Institute of Microsurgery on Extremities, Shanghai Jiao Tong University Affiliated Sixth People's Hospital; [3]Metabolic Bone Disease and Genetic Research Unit, Division of Osteoporosis and Bone Disease, Department of Endocrinology and Metabolism, Shanghai Jiao Tong University Affiliated Sixth People's Hospital, Shanghai 200233, P.R. China

Received June 15, 2017; Accepted February 28, 2018

DOI: 10.3892/ijmm.2018.3534

Abstract. Glucocorticoids (GCs) are the most common cause of atraumatic osteonecrosis of the femoral head (ONFH) because their effect compromises the osteogenic capability of bone marrow-derived mesenchymal stem cells (BMSCs). Valproic acid (VPA) is a widely used anti-epileptic and anti-convulsant drug. Previous studies have reported that VPA promotes osteogenic differentiation of MSCs *in vitro* and osteogenesis *in vivo* as a histone deacetylase (HDAC) inhibitor. The purpose of the present study was to investigate the efficacy of VPA as a precautionary treatment of ONFH after GC treatment in rats. *In vitro*, the effect of VPA, dexamethasone or a combination treatment of the two on the proliferation and osteogenic differentiation of human BMSCs was assessed using a Cell Counting Kit-8 and apoptosis assays, and by measuring the expression of proteins associated with osteogenesis. *In vivo*, a GC-induced ONFH model was established in rats and VPA was added during GC treatment to investigate the preventive effect of VPA against ONFH. Rat BMSCs were also extracted to investigate the osteogenic capacity. The results of micro-computed tomography scanning, angiography of the femoral head and histological and immunohistochemical analyses indicated that 11 of 15 rats induced with methylprednisolone (MP) presented with ONFH, while only 2 of 15 rats treated with a combination of MP and VPA developed ONFH. VPA produced beneficial effects on subchondral bone trabeculae in the femoral head with significant preservation of bone volume and blood supply, as well as improved osteogenic capability of BMSCs compared with those in rats treated with GC alone. In conclusion, VPA attenuated the inhibitory effect of GC on BMSC proliferation and osteogenesis by inhibiting apoptosis and elevating the expression of proteins associated with osteogenesis, which may contribute to the prevention of GC-induced ONFH in rats.

Correspondence to: Professor Chang-Qing Zhang, Department of Orthopaedic Surgery, Shanghai Sixth People's Hospital, Shanghai Jiaotong University, 600 Yishan Road, Shanghai 200233, P.R. China
E-mail: zhangcq@sjtu.edu.cn

Key words: valproic acid, osteonecrosis of the femoral head, glucocorticoid, mesenchymal stem cell, osteogenic differentiation

Introduction

Osteonecrosis of the femoral head (ONFH) is a refractory disease affecting young individuals, which is characterised by hip pain and dysfunction or even lameness (1,2). While several risk factors are known, glucocorticoid (GC) medication is thought to be the principle one, causing 10-30% of non-traumatic ONFH (3). GC has been widely used in the treatment of rheumatic and auto-immune diseases, and for chemotherapy and acute medical conditions, including traumatic spinal cord injury (4-7). Hence, ONFH is a potential complication for numerous patients receiving GC treatment. The pathogenesis of ONFH includes ischaemia, necrosis, repair and deformity in the femoral head (8-10). All of these changes occur sequentially, resulting in collapse of the femoral head. GC may cause ONFH through several mechanisms. First, a GC overdose often exerts adverse effects on the vascular system, including hypertension, atherosclerosis and coagulation abnormalities, leading to diminished blood supply in the femoral head (11,12). Secondary to GC administration, patients present with a decreased pool of mesenchymal stem cells (MSCs) in the proximal femur (13) and a reduced activity of MSCs (14). MSCs have a vital role in the osteonecrosis repair process. When osteonecrosis appears, fibrous tissue carrying undifferentiated mesenchymal cells invades the necrotic area and then initiates new bone formation; however, this is slower than the spread of fibrous tissue, therefore leading to incomplete reconstruction of the necrotic area (15-18). GC has been reported to inhibit the proliferation and osteogenic differentiation of MSCs. The inhibitive role of GC may be associated with the induction of apoptosis and downregulation of runt-elated transcription factor 2 (Runx2)/core-binding factor α1 (Cbfa1), which is considered to be important in osteogenesis, particularly for

the development of osteoblasts (19,20). Furthermore, MSCs extracted from steroid-induced ONFH patients have a compromised osteogenic ability, an elevated adipogenic ability and a lower proliferation rate (21-25). Therefore, the enhancement of proliferation and osteogenesis in bone marrow-derived MSCs (BMSCs) in patients receiving GC by other drugs may improve the repair process or even prevent ONFH.

Valproic acid (VPA) has been approved by the Food and Drug and Administration of the US to treat epilepsy for >20 years (26). It has been reported that VPA promotes the osteoblast differentiation and maturation processes through the regulation of cell histone acetylation (27,28). Histone acetylation is a reversible epigenetic process delicately modulated by histone acetyltransferases (HATs) and histone deacetylases (HDACs). HATs are responsible for histone hyperacetylation, resulting in relaxation of the chromatin structure, and allow the binding of DNA sequences with transcription factors, thereby activating transcription and downstream expression. Conversely, HDACs deacetylate histones and silence transcription, thereby counteracting the effects of HATs (29). This epigenetic regulation of gene expression has a dominant role in cell stemness, determination, commitment and differentiation (30-33). HDACs are mainly classified into 4 groups: Class I HDACs (1, 2, 3 and 8), class IIa HDACs (4, 5, 7 and 9), class IIb HDACs (6 and 10), class III HDACs (sirtuin-1 to -7) and a class IV HDAC (HDAC11) (34). VPA, a potent class I and II HDAC inhibitor (HDACi), has been reported to promote osteogenic differentiation in a number of cell types, including osteoblasts, BMSCs adipose-derived stem cells and dental pulp stem cells *in vitro* (27,35-38). *In vivo*, VPA promotes bone healing at its clinically applied concentration (39). GC treatment may have a systemic influence on the vascular system and BMSC pool (40,41). Thus, an increasing number of studies focus on systemic administration of drugs to prevent or treat ONFH (42-44).

To the best of our knowledge, the effect of VPA on BMSC proliferation and osteogenic differentiation upon GC treatment has remained elusive, as well as whether systemic administration of VPA may improve the osteogenic differentiation of BMSCs and thus prevent the occurrence of ONFH after GC administration. The results of the present study indicated that VPA reduces the inhibitive effect of GC on proliferation, apoptosis and osteogenic differentiation of BMSCs *in vitro* and prevents the occurrence of ONFH in rats.

Materials and methods

Cell culture. The present study was performed according to the principles of the Helsinki Declaration, and written informed consent was obtained from each patient. The experimental procedures were approved by the Ethical Review Board of Shanghai Jiaotong University Affiliated Sixth People's Hospital (Shanghai, China). BMSCs were isolated from human bone marrow harvested from patients suffering femoral neck fracture during hip arthroplasty surgery. The BMSCs were purified and cultured according to a previously published protocol by our group (45). BMSCs of passages 3-6 were used in all experiments. Patient consent was provided before any procedures were performed. BMSCs from proximal femurs of rats were extracted and cultured using the same methods.

Cell proliferation and apoptosis assay. First, the effect of VPA, dexamethasone (DEX) and a combination of the two drugs on BMSC proliferation and apoptosis was assessed. BMSCs were seeded in 96-well plates (3-wells per group) with the same number of cells and divided into 5 groups: i) Control; ii) VPA 0.5 mM; iii) VPA 1 mM; iv) VPA 2 mM; and v) VPA 5 mM. DEX at 10^{-5} M was selected due to its significant inhibitive effect on cell proliferation and osteogenesis reported in previous studies (46,47). In addition, the following DEX groups with or without VPA treatment were established: i) DEX; ii) DEX+VPA 0.5 mM; iii) DEX+VPA 1 mM; iv) DEX+VPA 2 mM; and v) DEX+VPA 5 mM.

The Cell Counting Kit-8 (CCK-8) assay was used according to the manufacturer's instructions at 24, 72, 120 and 168 h after BMSC adherence and the above treatments. At these time-points, 10 μl CCK-8 reagent was added into 100 μl of culture medium in each well, followed by incubation for another 3 h. The absorbance value was measured using a microplate reader (Bio-Rad Laboratories, Inc., Hercules, CA, USA) at 450 nm.

To evaluate the effect on apoptosis, BMSCs cultured with 5 mM VPA, DEX and DEX plus 5 mM VPA for 5 days were subjected to Annexin V-fluorescein isothiocyanate and propidium iodine double staining (Dojindo, Kumamoto, Japan), and the apoptotic rate was measured by flow cytometry according to the manufacturer's protocols.

Osteogenic induction assay. BMSC differentiation was initiated 48 h after the cells were plated, with the basic medium in each group supplemented with 10^{-2} M β-sodium glycerophosphate, 50 μg/ml L-ascorbic acid and 10^{-7} M DEX. The medium was changed every 3 days. First, the osteogenesis-associated mRNA levels of BMSCs treated with VPA alone for 7 and 14 days were measured via a polymerase chain reaction (PCR) assay. Next, BMSCs were osteo-induced with VPA at gradient concentrations for 7 and 21 days in a mineralisation assay. Subsequently, the effect of DEX in the presence or absence of VPA on BMSC osteogenesis and mineralisation was tested. For PCR and western blot assays, BMSCs were cultured for 7 days. For alizarin red S staining, BMSCs in each group were cultured for 21 days. Alkaline phosphatase (ALP) activity was measured after 14 days of osteo-induction.

Reverse transcription-quantitative PCR (RT-qPCR) analysis. Total RNA was extracted from osteogenic-induced BMSCs in each group with TRIzol reagent (Invitrogen; Thermo Fisher Scientific, Inc., Waltham, MA, USA). The RT reaction was performed using EasyScript one-step gDNA Removal and cDNA Synthesis Supermix (TransGen Biotech, Beijing, China) from 1 μg of total RNA according to the manufacturer's protocols. qPCR of type I collagen (COL I, ALP, osteocalcin (OCN) and Runx2 were performed with the TransStart Tip Green qPCR SuperMix (TransGen Biotech). The relative amount of mRNA was normalised to β-actin (48). The forward and reverse primers of each complementary (c)DNA were designed as follows: β-actin, 5'-GTCATCCATGGC GAACTGGT-3' and 5'-CGTCATCCATGGCGAACTGG-3'; Runx2, 5'-CCGAGACCAACCGAGTCATTTA-3' and 5'-AAG AGGCTGTTTGACGCCAT-3'; ALP, 5'-CAAGGATGCTGG GAAGTCCG-3' and 5'-CTCTGGGCGCATCTCATTGT-3';

OCN, 5'-CCCCCTCTAGCCTAGGACC-3' and 5'-ACCAGG TAATGCCAGTTTGC-3'; COL I, 5'-CAGCCGCTTCACCTA CAGC-3' and 5'-TTTTGTATTCAATCACTGTCTTGCC-3'. The PCR system was as follows: cDNA, 1 μl; double-distilled water, 3.4 μl; Tip Green qPCR SuperMix, 5 μl; passive reference dye (50X), 0.2 μl; forward primer (10 μmol/l), 0.2 μl; reverse primer (10 μmol/l), 0.2 μl. The total volume of the system was 10 μl. The reaction conditions were 95˚C for 30 sec initial denaturation, followed by 40 cycles of 95˚C for 5 sec and finally 60˚C for 30 sec. Furthermore, a 65-95˚C solubility curve was constructed.

Western blot analysis. Proteins were extracted with a cell lysis buffer (radioimmunoprecipitation assay lysis and extraction Buffer, Thermo Fisher Scientific, Inc.) supplemented with proteinase inhibitor (#78430; Thermo Fisher Scientific, Inc.), and the total protein concentration was detected with a bicinchoninic acid assay. Following denaturation at 95˚C for 5 min, 30-μg aliquots of protein were subjected to 10% SDS-PAGE and transferred to a polyvinylidene fluoride membrane (Merck KGaA, Darmstadt, Germany). After being blocked with 5% dried skimmed milk, the membranes were labelled with a primary antibody to COL I (ab138492), Runx2 (ab23981), ALP (ab186422) and β-actin (ab115777) (Abcam, Cambridge, UK) at a concentration of 1:1,000 at 4˚C overnight and then immersed in the secondary antibody working solution containing anti-rabbit immunoglobulin G (#14708; Cell Signaling Technology, Inc., Danvers, MA, USA) (1:1,000) at 37˚C for 1 h. After chemiluminescence staining (Pierce™ ECL, #32106; Thermo Fisher Scientific, Inc.) with a commercial assay, the target bands were detected with a gel image-processing system. The protein levels were normalised against β-actin. Histone extraction was performed according to the protocol of a previous study (35), and the membranes were incubated with primary antibodies to HDAC1 (AH379; Beyotime Institute of Biotechnology, Shanghai, China), HDAC2 (AH382; Beyotime Institute of Biotechnology), acetylated histone H3 (ac-H3) (#06-599; EMD Millipore, Billerica, MA, USA), ac-H4 (#06-598; EMD Millipore) and histone H4 (ab31830; Abcam), which was used as the loading control, at a concentration of 1:500 at 4˚C overnight. Proteins were detected after incubation with goat anti-rabbit IgG secondary antibody (1:1,000; #14708; Cell Signaling Technology, Inc.) at 37˚C for 1 h and visualized using chemiluminescence in the same way according to manufacturer's protocols mentioned above.

ALP activity assay. The osteogenic differentiation of human (h)BMSCs was evaluated by the ALP activity assay. After culture for 7 days, the cell layers were gently washed with cold PBS and lysed in 200 μl of 0.2% Triton X-100 for 30 min. The lysates were centrifuged at 20,000 x g for 15 min at 4˚C and sonicated. Next, 30 μl of the supernatant was mixed with 150 μl of the working solution (Nanjing Jiancheng Bioengineering Institute, Nanjing, China) according to the manufacturer's protocol. The formation of p-nitrophenol from p-nitrophenylphosphate, the substrate of ALP, was evaluated by measuring the absorbance at 405 nm with a microplate reader (Bio-Rad 680; Bio-Rad Laboratories, Inc.). The ALP activity was calculated by determining the ratio of the absorbance of the experimental samples to that of the standard and was expressed as mM of p-nitrophenol produced per minute per mg of protein.

Alizarin red S staining. After osteogenic induction for 21 days, cells in 48-well plates (3-wells in each group) were fixed with 4% paraformaldehyde for 20 min, then rinsed twice with PBS (pH 7.4) and stained with 40 mM alizarin red working solution for 10 min at room temperature. After being rinsed twice with PBS again, these cells were visualised under a light microscope. Subsequently, 100 mmol/l cetylpyridinium chloride was added to each well and semi-quantitative analyses were performed by measurement of optical density values at 560 nm.

Animal model and grouping. All animal experiments in the present study were approved by the Animal Care and Use committee of Shanghai Sixth People's Hospital, Shanghai Jiaotong University School of Medicine (Shanghai, China). A total of 36 Sprague Dawley (SD) rats (weight, 250-300 g, 7 weeks old) purchased from Shanghai Animal Experimental Centre, (Shanghai, China) were divided into 3 groups. Six rats in the control group received no treatment; 15 rats in the methylprednisolone (MP) group were intramuscularly injected with MP 20 mg/kg/day (49,50) for 3 continuous days per week over a period of 3 weeks (total MP, 180 mg/kg) to induce ONFH, and 15 rats in the MP+VPA group were intraperitoneally injected with 300 mg/kg VPA (51,52) once a day for 3 weeks in a row until MP injection was ceased. MP rather than DEX was selected, as it is more commonly used in the clinic.

Serum ALP activity. Blood samples of 1 ml were harvested randomly from 3 SD rats in each group on the last day of weeks 1, 2 and 3 after injection. Serum separation was performed by centrifugation at 300 x g for 15 min at 4˚C. The serum was then mixed with the working solution for the ALP activity assay (#A059-2; Nanjing Jiancheng Bioengineering Institute, Nanjing, China) and processed according to the manufacturer's protocol. The optical density values were measured at 405 nm with a microplate reader (Bio-Rad 680; Bio-Rad Laboratories, Inc.).

Micro-computed tomography (CT) scanning. To evaluate bone morphologic changes in the rats, the right femoral head of each rat was scanned with a micro-CT scanner (Skyscan 1176; Bruker MicroCT, Kontich, Belgium) at a resolution of 9 microns. Two-dimensional (2D) images were analysed using CTAn software (v.1.13; Bruker MicroCT). Primarily, the trabecular bone parameters of whole subchondral bone in the femoral head were measured. Specifically, the bone mineral density (BMD), bone volume per tissue volume (BV/TV) and trabecular thickness (Tb.Th) were quantified.

Angiography. After cardiac perfusion with heparinised saline, Microfil (MV-112; Flow Tech, Inc., Carver, MA, USA) was injected into the abdominal aorta until a constant outflow of the compound was observed from the abdominal vein. All the surgical steps were under anaesthesia after intraperitoneal injection of 4% chloral hydrate (360 mg/kg). Subsequently, the rats were stored at 4˚C overnight to ensure the polymerisation of the contrast agent. Femoral heads were fixed with 10%

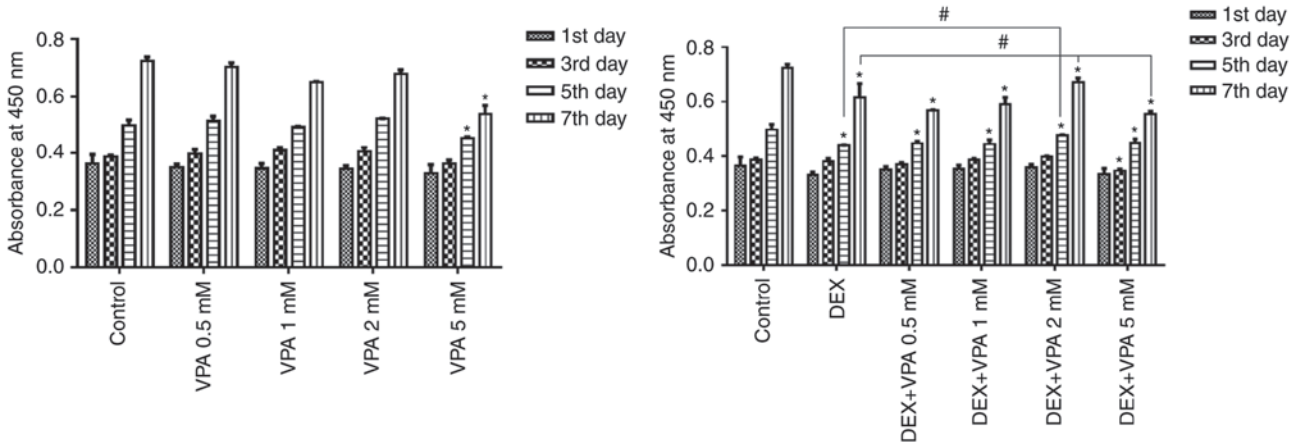

Figure 1. Effects of VPA, DEX and a combination of DEX and VPA on BMSC proliferation. After treatment of VPA, DEX and DEX plus different concentrations of VPA, the proliferation of BMSCs was detected with a Cell Counting Kit-8, and the results were expressed as the mean absorbance value ± standard deviation. *P<0.05 vs. control group; #P<0.05 vs. DEX group. BMSCs, bone marrow mesenchymal stem cells; DEX, dexamethasone; VPA, valproic acid.

formalin and decalcified with a 10% EDTA solution. Finally, the samples were scanned via micro-CT as described above.

Histological and immunohistochemical (IHC) analyses. After decalcification and paraffin embedding, femoral heads were sectioned at a thickness of 5 μm in the coronal plane. Certain sections were stained with haematoxylin and eosin (H&E) at room temperature for 5 min to evaluate the trabecular structure, while others were deparaffinised, subjected to antigen retrieval and incubated with anti-OCN (1:50; ab13420; Abcam), anti-Runx2 (1:200; ab23981; Abcam) and anti-vascular endothelial growth factor (VEGF; 1:50; BA0407; Boshide, Wuhan, China) primary antibodies at 4˚C overnight and then incubated with the Super Vison Polymer anti-rabbit lgG-HRP kit at 37˚C for 30 min according to the manufacturer's protocols (SV0002; Boshide). Staining was visualized with 3,3-diaminobenzidine and samples were counterstained with haematoxylin for 1 min at room temperature. Photomicrographs were acquired using a Leica DM 4000 (Leica Microsystems, Wetzlar, Germany).

Statistical analysis. SPSS 20.0 (IBM Corp., Armonk, NY, USA) was used to analyse the values in each group. Values are expressed as the mean ± standard deviation. Comparisons of data among the groups were performed using one-way analysis of variance with Student-Newman-Keuls post hoc analysis. P<0.05 was considered to indicate a statistically significant difference.

Results

VPA at a high concentration inhibits BMSC proliferation, while VPA at lower concentrations inhibits DEX-induced decreases in BMSC proliferation. The CCK-8 assay indicated that the amount of BMSCs in all groups gradually increased in a time-dependent manner, but proliferation was significantly repressed after incubation with 5 mM VPA and with 10^{-5} M DEX in the presence or absence of VPA. The BMSC proliferation rate was not significantly influenced by 0.5-2 mM VPA, but these concentrations of VPA attenuated the inhibitory effect on BMSC proliferation exerted by DEX in a dose-dependent manner, except for the 5-mM concentration of VPA, which decreased the proliferation compared with that in the groups treated with DEX alone (Fig. 1).

VPA decreases the apoptotic rate of BMSCs induced by DEX. The apoptosis assay indicated that DEX promoted cell apoptosis. The apoptotic cells in the DEX group was >40%, which was significantly higher than that in the control group (24.83%). Although 5 mM VPA inhibited BMSC proliferation, it exerted no significant effect on cell apoptosis. However, when 5 mM VPA was added to the DEX culture, the amount of apoptotic BMSCs was significantly reduced (Fig. 2).

VPA increases osteogenic differentiation and improves the osteogenic capacity of BMSCs compromised by DEX treatment by inhibition of HDAC activity. First, BMSCs were treated with different concentrations of VPA, and RT-qPCR analysis revealed that 1 mM VPA significantly increased the mRNA levels of Runx2, ALP, COL I and OCN after 7 days of culture. After osteogenic induction for 14 days, VPA at all concentrations promoted the expression of these osteogenesis-associated genes to varying degrees, while decreasing that of Runx2. The most efficacious concentration of VPA at 7 and 14 days was 1 mM (Fig. 3). Next, the protein expression of Runx2, COL I and ALP, as well as ALP activity, was investigated in the same treatment groups. The results indicated that VPA elevated ALP activity and the protein expression of ALP, COL I and Runx2 (Fig. 4A-C). With VPA treatment at 1 mM, a similar trend to that in ALP activity was observed regarding ALP expression (Fig. 4D). Given that 5 mM VPA caused a downward trend in proliferation, only the lower concentrations (0.5-2 mM) were added into osteogenic medium containing 10^{-5} M DEX, in which BMSCs were cultured for 7 days. The results indicated that DEX decreased the protein levels of Runx2, COL I and ALP in comparison with those in the control group, while the addition of 0.5 and 1 mM VPA enhanced the levels of all of these proteins to varying degrees. Specifically, 0.5 and 1 mM VPA recovered Runx2 expression to the same level as that in the control group, and rescued ALP expression. Furthermore, supplementation with 0.5 mM VPA gave rise to

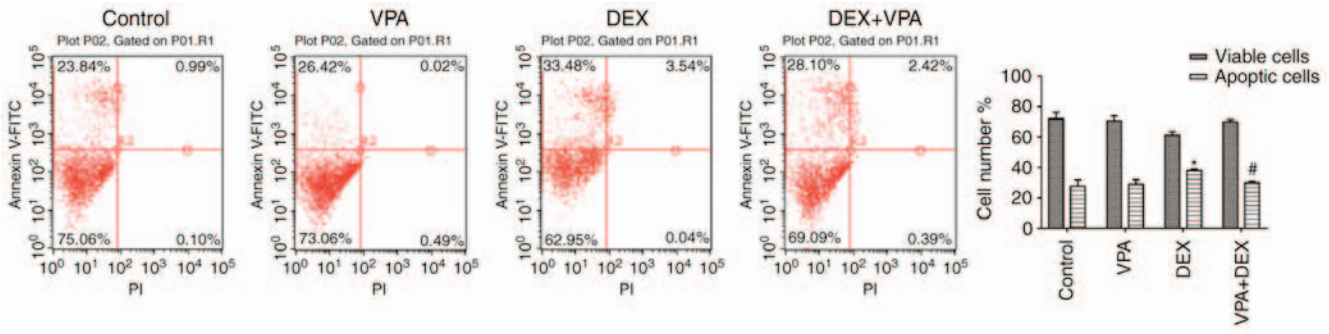

Figure 2. Effects of VPA, DEX and a combination of DEX and VPA on the apoptosis of BMSCs. After treatment with 5 mM VPA, DEX and DEX+5 mM VPA, the apoptotic rate of BMSCs was detected by flow cytometry after Annexin V-FITC and PI staining, and the apoptotic rates were calculated. *P<0.05, vs. the control, #P<0.05 vs. DEX group. FITC, fluorescein isothiocyanate; PI, propidium iodide; DEX group. BMSCs, bone marrow mesenchymal stem cells; DEX, dexamethasone; VPA, valproic acid.

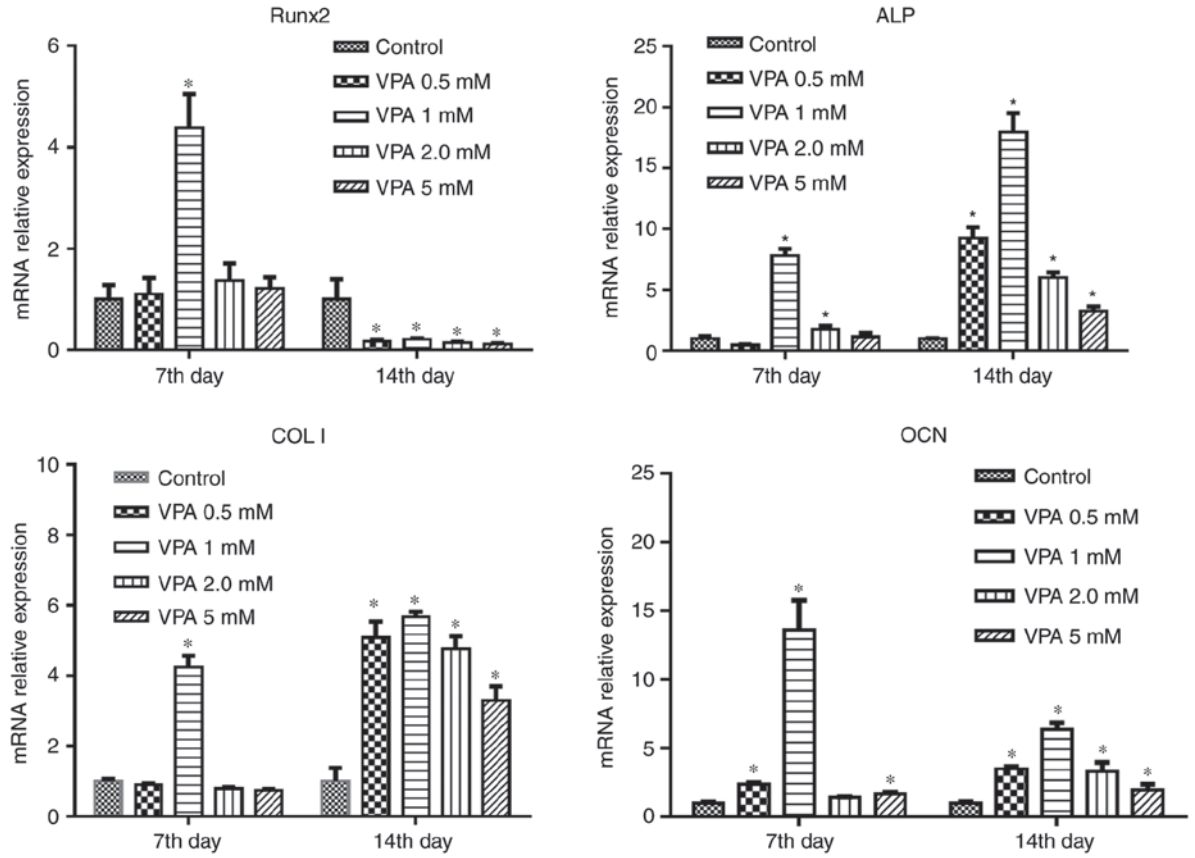

Figure 3. Expression of genes associated with osteogenesis in BMSCs treated with various concentrations of VPA. The mRNA expression of Runx2, ColI, ALP and OCN in BMSCs was detected by polymerase chain reaction analysis. Values are expressed as the mean ± standard deviation (n=3). *P<0.05 vs. control group. BMSCs, bone marrow mesenchymal stem cells; VPA, valproic acid; Runx2, runt-related transcription factor 2; ALP, alkaline phosphatase; OCN, osteocalcin; ColI, type I collagen.

significantly higher expression levels of COL I than those in the control and DEX groups. However, the addition of 2 mM VPA repressed the expression levels of Runx2, COL I and ALP (Fig. 5A). Considering that VPA is an HDACi, the protein expression of HDAC1 and HDAC2 as class I HDACs as well as the levels of ac-H3 and ac-H4 were measured. The results indicated that the two HDACs were lowered in all experimental groups, including the DEX and DEX+VPA groups, while ac-H3 and ac-H4 were lowered in the DEX group and upregulated with the addition of 0.5 and 1 mM, but not 2 mM VPA (Fig. 5B and C). Similarly, the mRNA levels of Runx2 and COL I were significantly lowered by DEX and elevated by the addition of VPA. Although DEX increased ALP, even higher ALP levels were observed after the addition of VPA. Likewise, 1 mM VPA exerted the greatest effect on COL I, Runx2 and ALP gene expression. However, VPA did not rescue the lowered OCN expression under DEX treatment (Fig. 6).

VPA promotes bone mineralisation and improves mineralisation compromised by DEX treatment. Alizarin red

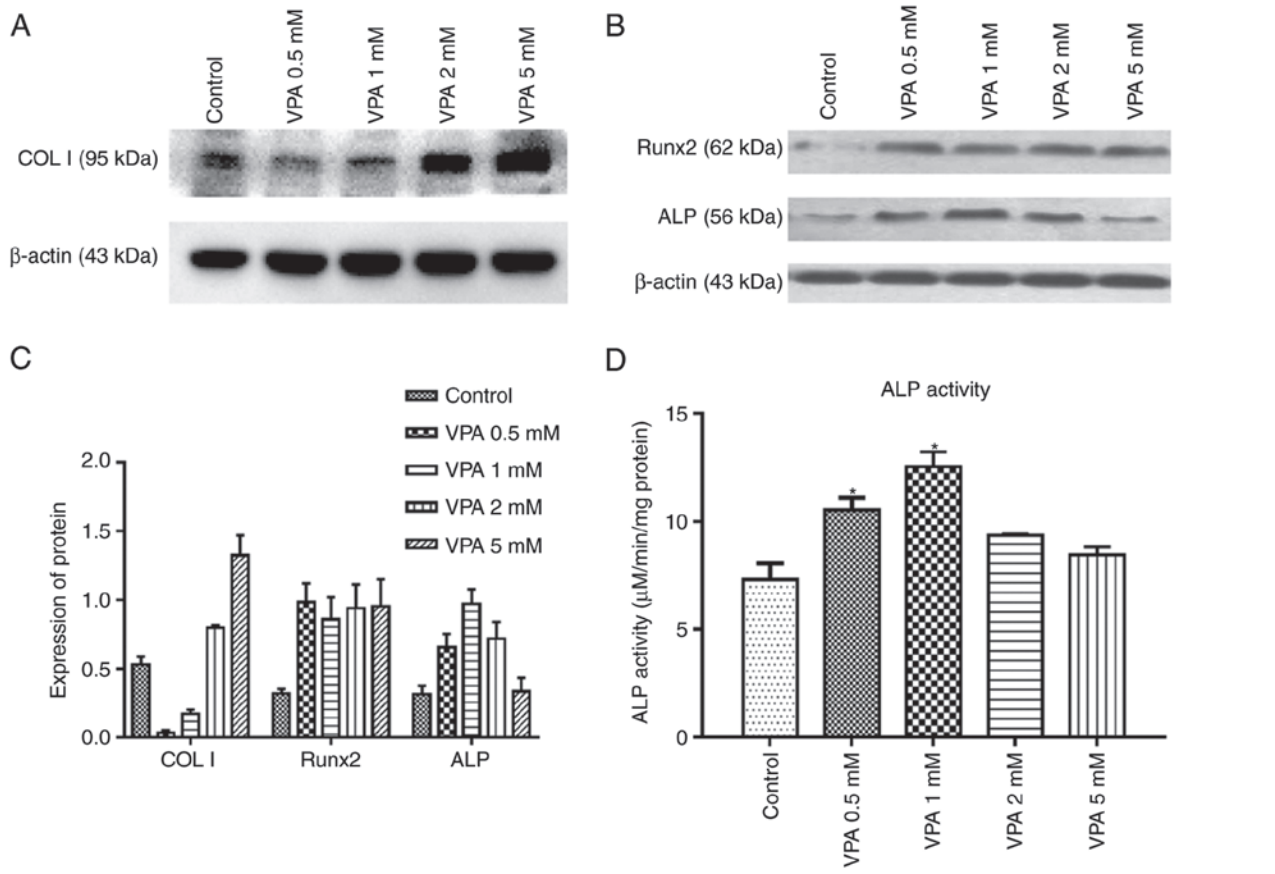

Figure 4. Expression of proteins associated with osteogenesis and ALP activity in BMSCs treated with various concentrations of VPA. (A-C) Protein expression of ColI, Runx2 and ALP during osteogenic induction were measured by western blot analysis. (D) ALP activity was assessed in BMSCs treated with VPA during osteogenic induction. Values are expressed as the mean ± standard deviation (n=3). *P<0.05 vs. control group. BMSCs, bone marrow mesenchymal stem cells; VPA, valproic acid; Runx2, runt-related transcription factor 2; ALP, alkaline phosphatase; OCN, osteocalcin; ColI, type I collagen.

S staining was used to assess calcium deposition, a characteristic of late-stage osteogenic differentiation of BMSCs. Fewer calcium deposits in the DEX group compared with those in the control group were observed, while more deposits were visible after VPA treatment. In addition, supplementation of VPA in addition to DEX significantly improved the mineralisation of BMSCs in comparison with DEX treatment alone (Fig. 7A). The staining eluate was then harvested with 1 ml cetylpyridinium chloride and the absorbance values were measured at 560 nm. The quantified results indicated the same trend as that of the microscopic views presented (Fig. 7B).

VPA increases serum ALP in rats treated with MP. Within the 3 weeks of the animal experiment, serum ALP activity in the MP group was highest in the first week. At 1 week, it was also significantly higher than that in the MP+VPA group. However, ALP activity in the MP group waned in the following 2 weeks and became lower than that in the control. Of note, with the addition of VPA, ALP activity was rescued to the level of the control in the second week, while this effect was attenuated but still significant in the third week (Fig. 8).

VPA improves subchondral bone formation under MP treatment. The trabecular changes in the subchondral area of the femoral heads were detected by micro-CT scan at 6 weeks after the first injection of MP. A total of 11 rats in the MP group exhibited visible osteonecrosis of the femoral head in the micro-CT images, while only 2 rats in the MP+VPA group had obvious osteonecrosis (Fig. 9A). The BMD of the rats in the MP group was 0.27±0.01 g/cm^3, which was significantly lower than that in the control group (0.61±0.01 g/cm^3), while supplementation with VPA significantly increased the BMD of the area to 0.43±0.01 g/cm^3. In addition, a similar effect was identified regarding the BV/TV and Tb.Th among these 3 groups of rats (Fig. 9B).

Similar to the micro-CT results, H&E staining of subchondral bone tissue revealed typical signs of osteonecrosis. Specifically, at low magnification, the MP group exhibited amorphous substance in the inter-trabecular spaces with few normal haematopoietic and fat cells on H&E staining. The trabeculae decreased in volume and became thinner in disarray and pale in staining in comparison with the control. At a magnification of x100, diffuse karyolytic and karyorrhectic nuclei of osteocytes were identified, and the marrow of amorphous matter was lacking normal cell nuclei, where there were mainly karyorrhectic and pyknotic speckles, revealing coagulation necrosis of the fatty hematopoietic tissue of the marrow. Furthermore, the ingrowth of fibrous tissue, a characteristic property of the repair process, was observed in this stage. However, with supplementation of VPA, no obvious necrotic area was present (Fig. 10A). The present study further assessed OCN expression as a marker of mature bone by IHC

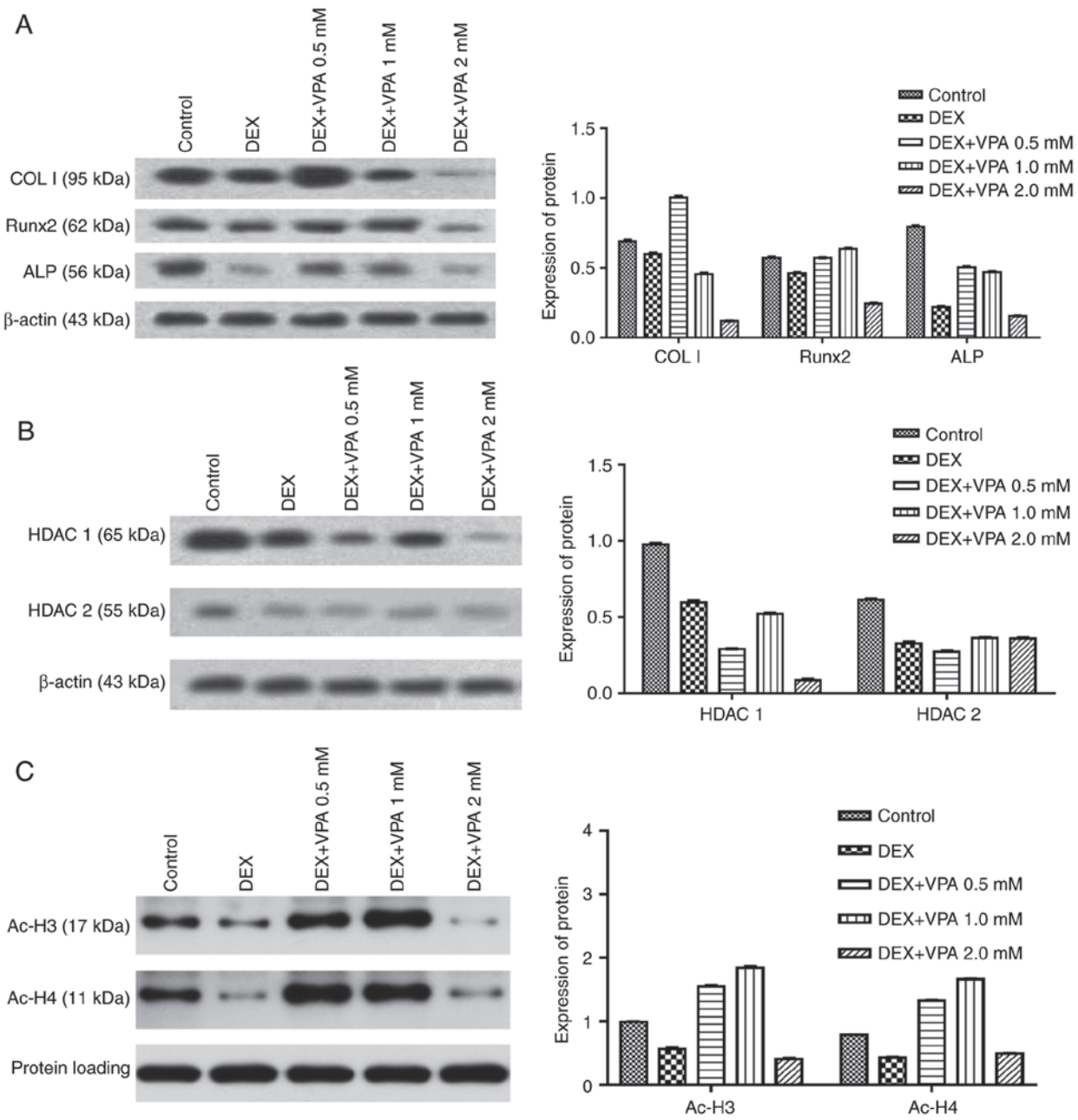

Figure 5. Expression of proteins associated with osteogenesis in BMSCs treated with various concentrations of VPA in combination with DEX. (A) Protein expression of Runx2, ColI and ALP in BMSCs. (B and C) The protein expression of HDAC1 and -2, ac-H3 and ac-H4. DEX, dexamethasone; BMSCs, bone marrow mesenchymal stem cells; VPA, valproic acid; Runx2, runt-related transcription factor 2; ALP, alkaline phosphatase; OCN, osteocalcin; ColI, type I collagen; HDAC, histone deacetylase; ac-H3, acetylated histone H3.

staining. The results indicated almost no positive area in the necrotic part of the subchondral bone after MP treatment, while the control and MP+VPA groups featured widespread OCN-expressing cells in the same area (Fig. 10B).

VPA preserves the blood supply to the femoral head. To detect the blood supply to the femoral head in the present study, micro-angiography of the femoral head was performed by perfusing the vessels with Microfil and observing them by micro-CT. The reconstructed 3D micro-CT images exhibited disrupted blood supply in the femoral head in the MP group, with vascularisation blocked around the femoral neck. However, the main vessel distributing to the femoral head in rats treated with MP+VPA was preserved (Fig. 11A). Correlation of micro-CT images and H&E staining revealed structural trabeculae in the vascularised area of the femoral heads. By contrast, the devascularised area displayed a lack of trabeculae and was referred to as the necrotic area. The vascularisation of the subchondral area of the femoral head was further detected by IHC analysis of VEGF. Nearly no staining for VEGF was observed in the subchondral bone area in the MP group, while a stained area was observed in the marrow cavity around the trabeculae in the MP+VPA and control groups (Fig. 11B).

VPA promotes the osteogenic capacity of BMSCs in rats. The BMSCs were subjected to osteogenic induction for

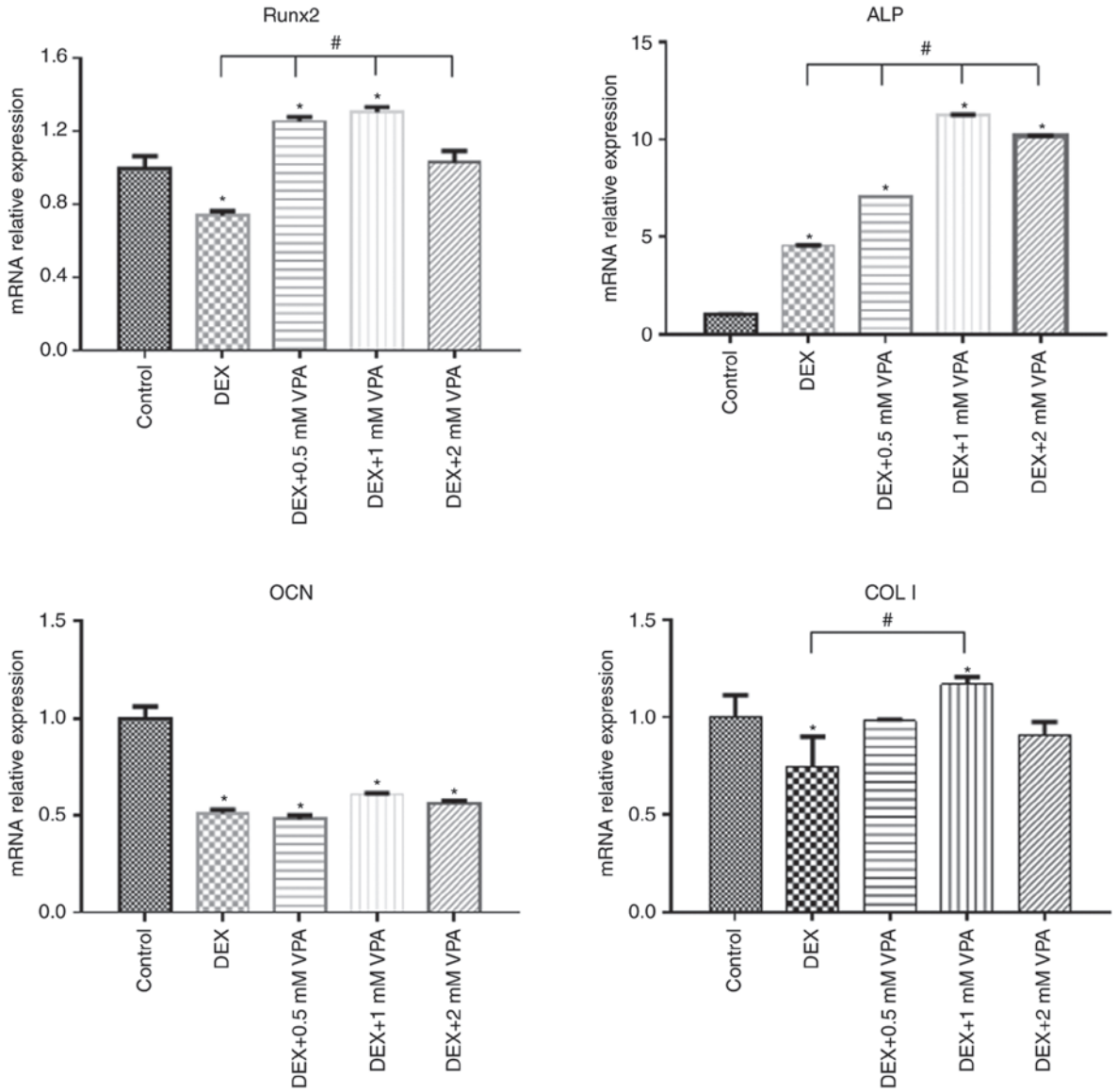

Figure 6. Expression of genes associated with osteogenesis in BMSCs treated with various concentrations of VPA in combination with DEX. The mRNA expression of Runx2, COL I, ALP and OCN in BMSCs was detected by polymerase chain reaction analysis. Values are expressed as the mean ± standard deviation (n=3). *P<0.05 vs. control group; #P<0.05 vs. DEX group DEX, dexamethasone; BMSCs, bone marrow mesenchymal stem cells; VPA, valproic acid; Runx2, runt-related transcription factor 2; ALP, alkaline phosphatase; OCN, osteocalcin; ColI, type I collagen.

3 days after being extracted from the proximal femurs of rats from each group and cultured for 3-5 passages. Western blot analysis was performed to measure the expression of Runx2 directly influenced by VPA as reported in previous studies (53), as well as ALP, its downstream protein. The results indicated that Runx2 and ALP expression were lowered in the MP group and improved with the addition of VPA (Fig. 12).

Discussion

ONFH is a common side effect of exogenous GC usage. One of the major underlying mechanisms is the inhibitory role of GCs in the osteogenesis of BMSCs, which influences the repair process of osteonecrosis. High doses of GCs may affect numerous processes involved in the differentiation of BMSCs. GCs may downregulate the expression of Runx2/Cbfa1, the key factor associated with osteogenic differentiation and maturation of osteoblasts (54). Several studies have indicated that GC antagonises Runx2 and subsequently compromises the expression of ALP, osteopontin and OCN in MSCs, resulting in inhibition of bone remodelling and fracture healing (19,55,56). The repair process is initiated when osteonecrosis takes place and is gradually outpaced by the proliferation of fibrous tissue, leading to incomplete reconstruction of the necrotic area devastated by the ceased blood supply. The ceased blood supply due to injury of vessels distributing to the femoral head is also attributed to failure of tissue reconstruction in the necrotic area. Consequently, the approach to prevent ONFH is more promising than to treat it, avoiding the loss of vessels that contributes to necrosis, which was applied in the present study.

VPA is an effective and widely used antiepileptic drug, which has been reported to influence osteogenesis as an

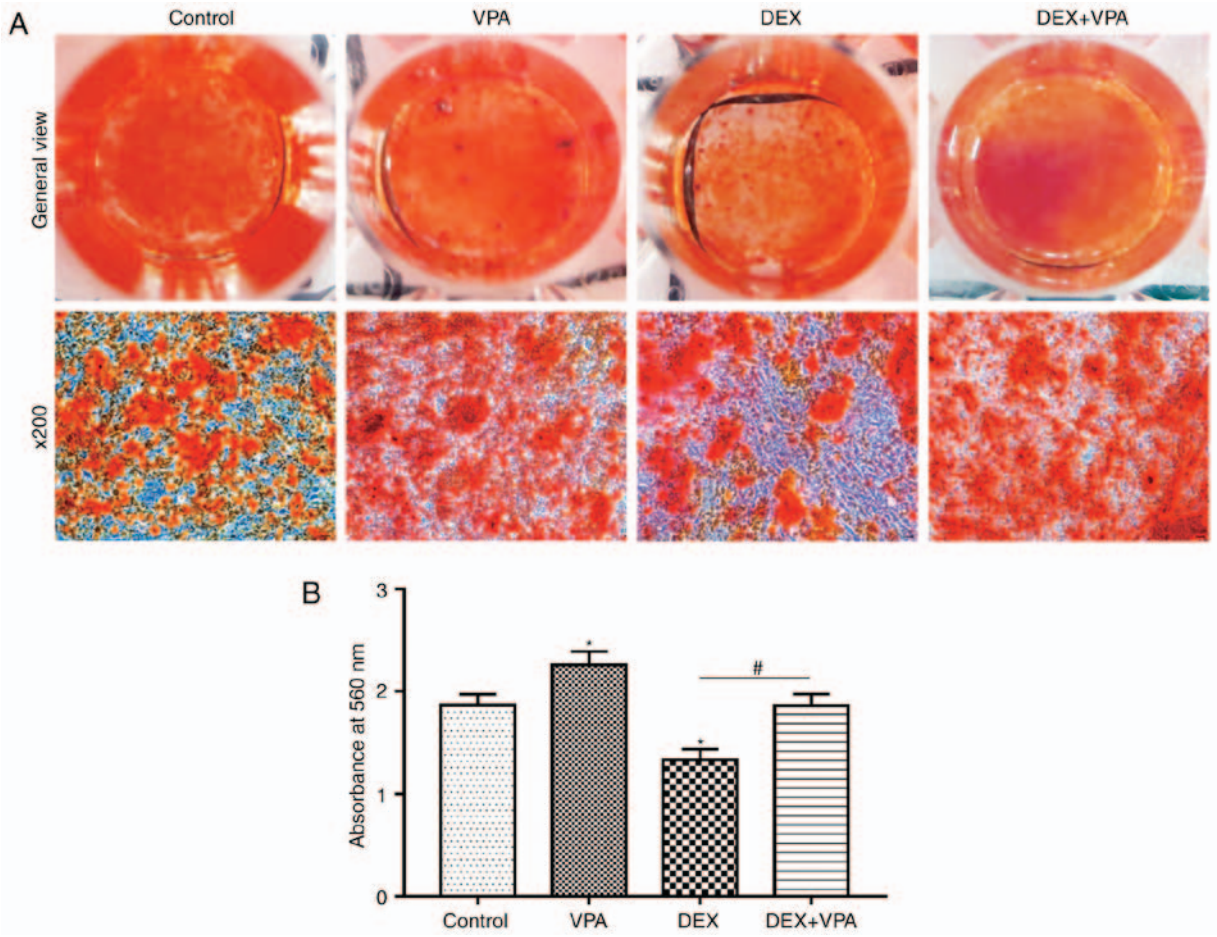

Figure 7. Effects of VPA, DEX and DEX+VPA on osteogenic differentiation of BMSCs. (A) Alizarin red S staining of BMSCs exposed to VPA, DEX and DEX plus 1 mM VPA during osteogenic differentiation (magnification, x200). (B) Quantification of alizarin red S staining was performed by measurement of the cetylpyridinium chloride eluate and presented as absorbance values at 560 nm. Values are expressed as the mean absorbance value ± standard deviation. *P<0.05 vs. control group; #P<0.05 vs. DEX group. DEX, dexamethasone; BMSCs, bone marrow mesenchymal stem cells; VPA, valproic acid.

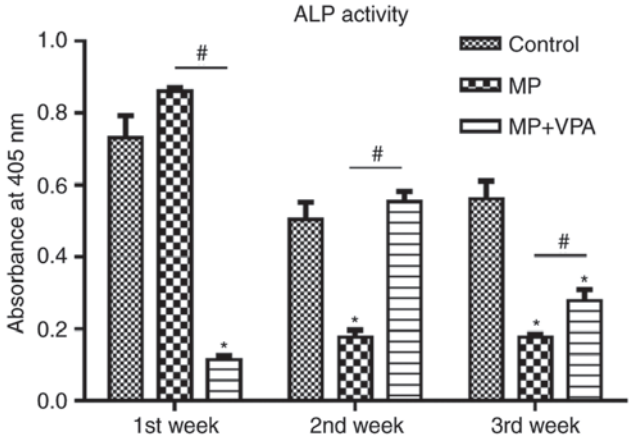

Figure 8. Analysis of serum ALP in Sprague Dawley rats. ALP activity was measured at 1, 2 and 3 weeks after injection of MP with or without VPA. Values are expressed as the mean absorbance value ± standard deviation. *P<0.05 vs. control group; #P<0.05 vs. MP group. VPA, valproic acid; ALP, alkaline phosphatase; MP, methylprednisolone.

HDACi (26). HDACis have been demonstrated to enhance osteoblast differentiation *in vitro* (34,53,57) and new bone formation *in vivo* (37,39). To the best of our knowledge, the present study was the first to indicate that VPA attenuates the inhibitive effect of GCs on the osteogenic differentiation of BMSCs, and that systemic injection of VPA prevents GC-induced ONFH in rats.

First, the effect of VPA alone on BMSC viability and apoptosis was observed. The results indicated that concentrations of VPA as high as 5 mM inhibited BMSC proliferation after 7 days of incubation, while VPA concentrations of 0.5-2 mM did not significantly influence BMSC proliferation. Hatakeyama *et al* (58) reported that (0.625-6.25 mM) VPA inhibited the proliferation of mouse embryonic stem cells. Lee *et al* (35,38) also reported that the proliferation of adipose-derived stem cells decreased in a dose-dependent manner after VPA treatment at 0.4-10 mM, but the extent of inhibition was not as great in umbilical cord blood-derived stem cells, displaying a significant decrease only with 10 mM VPA. The decrease in cell proliferation in the presence of high concentrations of VPA may be associated with cell apoptosis or cell cycle arrest. Lee *et al* (35,38) reported that the G2/M phase population of the cells was increased by VPA in a dose-dependent manner, while no increase in the sub-G1 phase was observed, demonstrating that the decrease in proliferation by VPA was not due to promoting apoptosis. In line with this, the present results also indicated that VPA concentrations as high as 5 mM inhibited the proliferation of BMSCs, but did

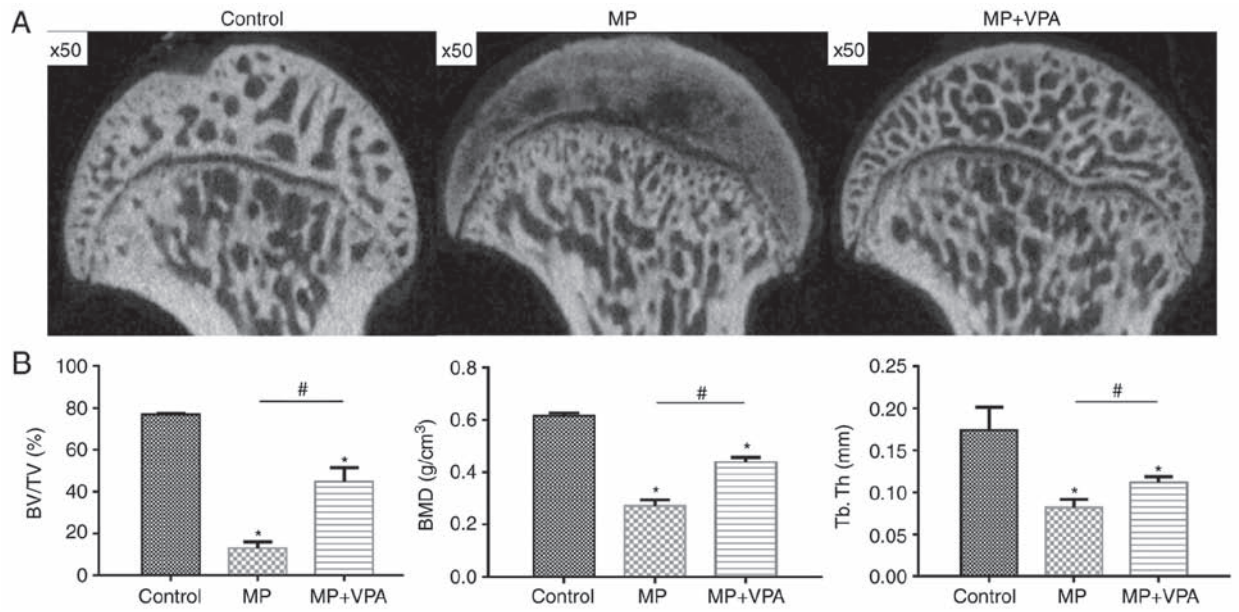

Figure 9. Micro-computed tomography evaluation of the subchondral trabeculae of the femoral heads. (A) 2-dimensional images of the coronal section of the femoral heads in each group. (B) Morphometric analysis provided trabecular parameters of the whole region of the subchondral bone of the femoral heads (magnification, x50). *P<0.05 vs. control group; #P<0.05 vs. MP group. VPA, valproic acid; MP, methylprednisolone; BMD, bone mineral density; BV/TV, bone volume per tissue volume; Tb.Th, trabecular thickness.

not significantly affect cell apoptosis. Accordingly, VPA may cause cell cycle arrest rather than cell apoptosis. Furthermore, cycle arrest is a prerequisite for cell differentiation, and thus, it is possible that VPA influences the osteogenic differentiation of BMSCs (58,59). However, in the present study, monotreatment with DEX significantly inhibited BMSC proliferation, while this effect was attenuated by co-treatment with 0.5-2 mM VPA. In a cell apoptosis assay, the percentage of apoptotic cells increased under DEX treatment, but improved after addition of 5 mM VPA. DEX has been reported to promote apoptosis of several types of stem cell (60-63). However, VPA may be able to hamper this negative effect of DEX by inducing cell cycle arrest, which requires further study. Taken together, the results of the present study suggested that low concentrations of VPA (0.5-2 mM) do not significantly influence BMSC proliferation and attenuate the negative effect on proliferation exerted by DEX. The underlying mechanisms may include a reduction of DEX-induced cell apoptosis by VPA.

Next, the effect of VPA on osteogenic differentiation of BMSCs was assessed. The results indicated that VPA alone promoted ALP, COL I, Runx2 and OCN mRNA expression. Specifically, BMSCs treated with 1 mM VPA for 7 days exhibited the highest osteogeneis-associated gene expression, while all concentrations of VPA significantly elevated these genes after 14 days of incubation, with the exception of Runx2. Runx2 expression was gradually reduced along with osteoblast maturation, and mature osteoblasts do not contain significant amounts of Runx2 protein (64). Hence, it is possible that VPA accelerated the osteogenic differentiation process of BMSCs, leading to a reduction of Runx2, but an elevation of COL I, ALP and OCN, all of which are expressed in mature osteoblasts. Similar results were obtained for the protein expression of ALP, COL I and Runx2, as well as for ALP activity. VPA at a concentration of 1 mM was selected due to its efficacy in the mineralisation assay, resulting in the promotion of calcium nodule deposition. All of the present results indicated that VPA promotes osteogenic differentiation of BMSCs.

DEX has been reported to inhibit osteogenic differentiation and bone formation *in vitro* and *in vivo* (19,55). The present study indicated that DEX inhibited COL I, Runx2 and ALP protein expression after osteogenic induction of BMSCs for 7 days. This inhibition was abrogated or attenuated by co-treatment with 0.5 and 1 mM of VPA for Runx2 or ALP, respectively. In addition, 0.5 mM VPA reversed the inhibitory effect of DEX on COL I, resulting in expression levels above those in the control group. Similar results were obtained for the mineralization of hBMSCs, manifesting in a protective effect of VPA on calcium deposition on BMSCs in the presence of DEX. Likewise, the gene expression of Runx2 and COL I was downregulated by DEX and reversed by the addition of VPA, and ALP expression exhibited the highest level with the addition of 1 mM of VPA. However, the lowered gene expression of OCN was not improved with the addition of VPA. Rimando *et al* (65) used high concentrations of DEX (10^{-5} M) for long-term treatment (7 days) of BMSCs and identified glucocorticoid receptor (GR)-HDAC6 complex as the repressor of the promoter region of OCN, leading to the downregulation of OCN mRNA. However, VPA inhibits class I HDACs more efficiently than class II HDACs, e.g., HDAC5 and -6 (27). It is possible that VPA at concentrations of 0.5-2 mM is not sufficient to inhibit HDAC6 to improve OCN mRNA expression. Consistent with the results of previous studies (66-71), the present study also indicated that VPA and DEX significantly inhibit HDAC1 and -2 expressions in BMSCs. Previous studies have demonstrated that GR elements are located in the promoter of the HDAC2 gene and that DEX treatment for 7 days reduced GR expression (66,67). Accordingly, HDAC2 expression may be lowered by DEX. DEX also affects histone acetylation. DEX acts by binding

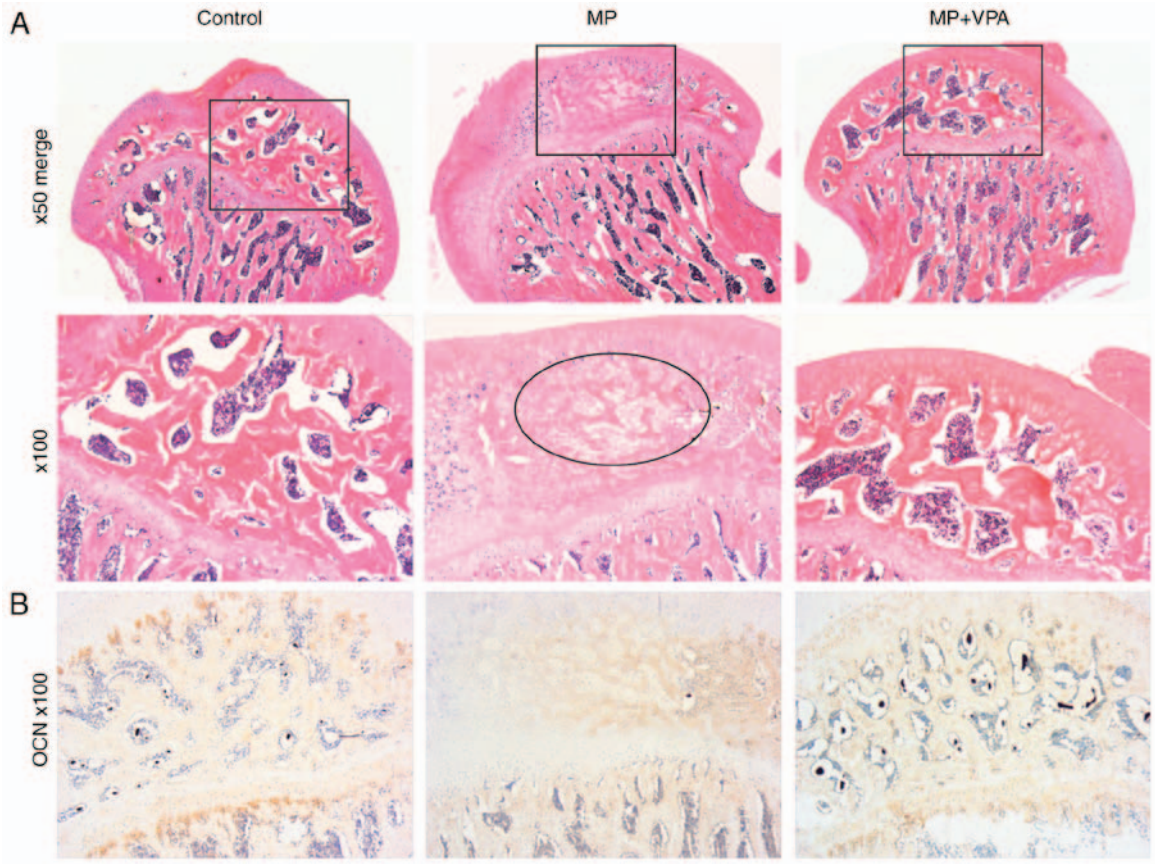

Figure 10. Histological analysis of paraffin sections of the femoral heads. (A) Representative images of H&E-stained coronal sections of femoral heads in each group. The rectangle refers to a part of the subchondral bone area (magnification, x50 and x100). At x100 magnification, the ellipses indicate the necrotic area, including karyolysis, karyorrhectic osteocytes, marrow necrosis and fibrous invasion. (B) Representative immunohistochemical staining images for OCN in the coronal sections of femoral heads in each group (magnification, x100). OCN, osteocalcin; VPA, valproic acid; MP, methylprednisolone.

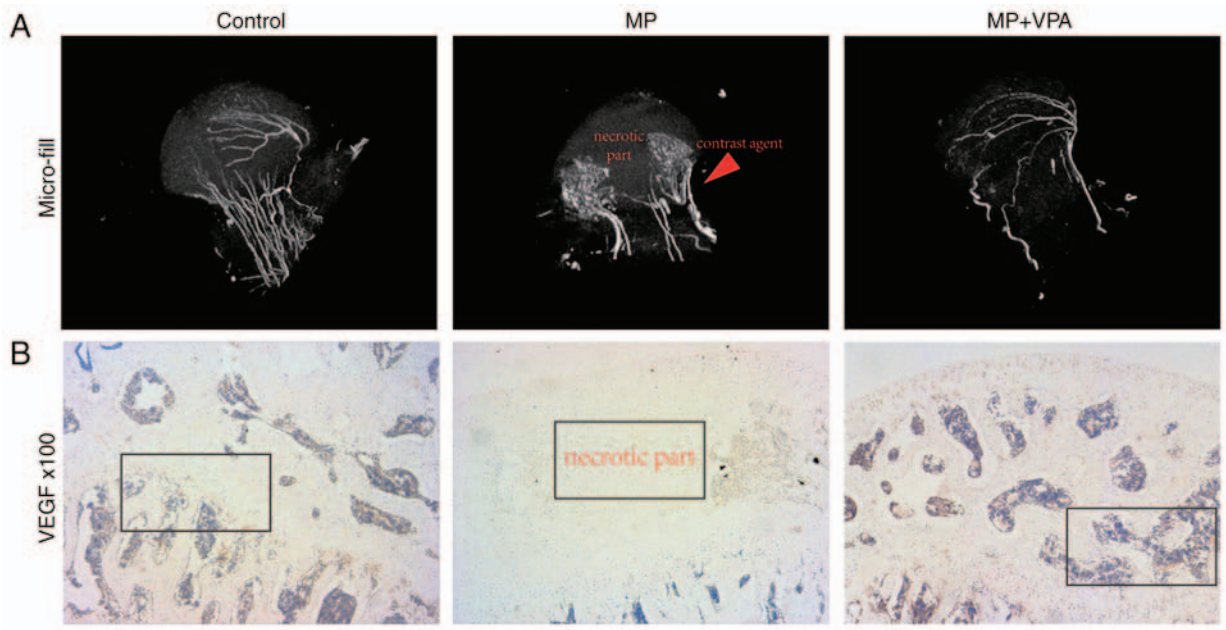

Figure 11. Evaluation of blood supply and vascularisation preservation in femoral heads. (A) Representative 3-dimensional micro-angiography images of femoral heads in each group processed by micro-computed tomography (magnification, x25). (B) Representative images of immunohistochemical staining for VEGF in the femoral heads of each group (magnification, x100). VEGF, vascular endothelial growth factor; VPA, valproic acid; MP, methylprednisolone.

to GR, which, upon activation, translocates to the nucleus and either increases or decreases gene expression (68). DEX has been reported to inhibit Runx2 expression by recruiting HDAC1 to the Runx2 promoter, which then mediates the

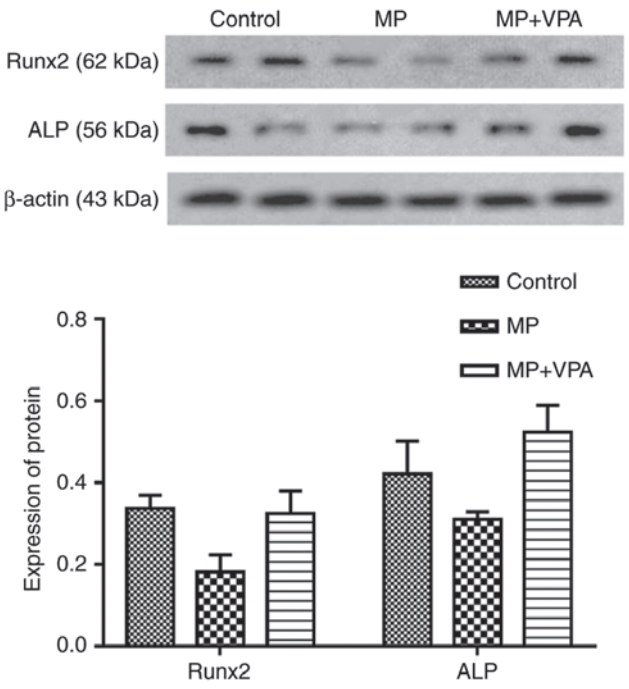

Figure 12. Expression of proteins associated with osteogenesis in rat BMSCs. The protein expression of Runx2 and ALP in rat BMSCs was detected by western blot and image analyses. Values are expressed as the mean ± standard deviation (n=3). *P<0.05 vs. control group; **P<0.05 vs. MP group. VPA, valproic acid; MP, methylprednisolone; BMSCs, bone marrow mesenchymal stem cells; Runx2, runt-related transcription factor 2; ALP, alkaline phosphatase.

deacetylation of histone H4 and downregulates Runx2 expression (69). In addition, the complex of DEX and GR recruits HDAC2 to the complex of nuclear factor-κB and activator protein 1 and reduces the associated inflammatory cytokine expression (70,71). The results of the present study also indicate that the levels of ac-H3 and ac-H4 were lower with DEX treatment alone than with the addition of VPA. Although DEX lowered the expression of HDAC1 and -2, as VPA did, the present results indicated that DEX did not have the same inhibitory effect on HDAC activity as VPA did. This may be the reason for DEX inhibiting osteogenic differentiation, and the addition of VPA may improve or reverse this inhibitory effect. As stated above, DEX inhibits osteogenic differentiation by binding to the promoter of Runx2 with GR, recruiting HDACs and bringing transcription to an end. Consequently, VPA has a beneficial effect on osteogenic differentiation inhibited by DEX, which may be explained by the inhibition of HDACs and rendering of histone acetylation, giving rise to initiation of Runx2 expression.

The present study hypothesized that VPA has a beneficial effect against GC-induced ONFH. In a previous study, Xu *et al* (35) reported that pre-treatment of mouse adipose-derived stem cells with VPA for 2 days produced an increased amount of bone formation after injection into bone defect areas. Rashid *et al* (39) demonstrated that intraperitoneal injection of VPA for 1 week accelerated the healing of maxillary bone cavities. To the best of our knowledge, no previous *in vivo* experiment has been performed to assess the preventive effect of VPA against GC-induced ONFH. GC-induced ONFH was successfully achieved in rats by injection of 20 mg/kg MP on 3 consecutive days over 3 weeks. Previously, animal models of ONFH have been established using a combination of 20 mg/kg MP and 2 mg/kg lipopolysaccharide (72-74), as LPS causes vasculitis, which occurs in most autoimmune diseases (75). However, not all patients receiving GC treatment are diagnosed with autoimmune diseases, e.g. those with spinal cord injury. Accordingly, it is better to establish an animal model of ONFH by induction with MP only to study GC-induced ONFH. The GC-induced rat model of ONFH has been successfully established in previous studies (49,50). In the present study, this ONFH rat model exhibited characteristics of classically-defined necrosis on histology with karyolytic and karyorrhectic osteocytes; it also featured necrotic marrow filled with acellular substance or fibroblasts invasion, and sinusoidal vessels devoid of red blood cells, demonstrating that devascularisation and necrosis had occurred in the femoral head. Of the rats that had received MP injection, a randomly selected 50% were simultaneously administered 300 mg/kg VPA once a day for 3 weeks with no intermittence, as administration of 250-300 mg/kg VPA has been reported to cause HDAC inhibition and improve functional recovery in stroke (76), nerve injury (77), retinal ischaemic injury (78) or survival of haemorrhagic shock (79). However, it remains elusive whether 300 mg/kg of VPA is the optimal dose, e.g. whether larger doses would increase the efficacy or whether smaller doses would suffice, particularly in long-term treatment periods of ≥3 weeks. Therefore, the dose-dependent effect on the prevention of GC-induced ONFH will be assessed in a future study.

In the present study, blood samples were collected from the experimental rats for measurement of serum ALP activity, which reflects the process of bone formation in general. The results indicated that MP+VPA attenuated the suppression of ALP activity caused by MP during the second and third weeks. VPA treatment enhanced the serum ALP levels, which may explain for how VPA attenuates the inhibitory effect of MP on ALP activity (80). However, serum ALP is an indicator of bone formation rather than osteonecrosis progression (81-83). The bone density of the femoral head was then measured, and histological and angiographic analyses were performed. Overall, 11 out of 15 rats that had received MP treatment presented with ONFH, but it only occurred in 2 out of 15 rats subjected to MP+VPA treatment. The results of the micro-CT scanning indicated that VPA yielded a greater preservation of trabeculae and bone volume in animals treated with MP (MP+VPA group). On the contrary, no normal-shaped trabeculae were observed in the subchondral area, which was only filled with a silt-like substance in single treatment of MP. On histological analysis, the femoral heads exhibited no apparent necrotic area in the group subjected to VPA treatment, with evenly distributed expression of OCN along the trabeculae, indicating that VPA treatment preserves a relatively large amount of mature bone under MP challenge. The major blood supply into the femoral head was also preserved in the VPA group, and as in the control group, an area of VEGF-expressing tissue was observed in the marrow cavity, indicating that VPA may be able to protect vessels as well. A further study on the effect of VPA against MP- or DEX-induced vessel deficits will be performed in the future. Finally, BMSCs were collected from rats in each group and western blot analysis indicated that the protein expression of

Runx2 and ALP was higher in the MP+VPA group compared with that in the MP group, indicating that the osteogenic capacity may have been improved by co-treatment with VPA, as indicated in the *in vitro* experiments. It may also be possible to prevent ONFH by improvement of the osteogenic capacity of BMSCs.

In summary, the present study reported that VPA enhanced the osteogenic differentiation of BMSCs, and attenuated the negative effect of GCs on BMSC proliferation, apoptosis and osteogenic differentiation. To the best of our knowledge, the present study was also the first to apply VPA as a preventive agent against GC-induced ONFH. The present results demonstrate that VPA is a promising drug for preventing ONFH, possibly via the enhancement of the osteogenic differentiation of BMSCs.

Acknowledgements

Not applicable.

Funding

Financial support from the National Natural Science Foundation of China (grant no. 81371959), Ministry of Major Disease Joint Program of Shanghai Health System (grant no. 2014ZYJB0301).

Availability of data and materials

The analyzed data sets generated during the study are available from the corresponding author on reasonable request.

Authors' contributions

DZ was responsible for designing the concept, acquisition of data, analysis and interpretation and manuscript writing. CZ and YF contributed to the design, analysis and interpretation. YC analysed and interpreted the data and animal experiments. JY, ST and SG were involved in the experimental method optimisation. ZW contributed to the Micro-CT scanning and analyses. Each author read and approved the final version of the manuscript.

Ethical approval and consent to participate

The present study was performed according to the principles of the Helsinki Declaration, and written consent was obtained from each patient. The experimental procedures were approved by the Ethical Review Board of Shanghai Jiaotong University Affiliated Sixth People's Hospital (Shanghai, China). Patient consent was provided before any procedures were performed.

Consent for publication

Not applicable.

Competing interests

The authors declare that they have no competing interests.

References

1. Assouline-Dayan Y, Chang C, Greenspan A, Shoenfeld Y and Gershwin ME: Pathogenesis and natural history of osteonecrosis. Semin Arthritis Rheum 32: 94-124, 2002.
2. Mont MA, Jones LC and Hungerford DS: Nontraumatic osteonecrosis of the femoral head: Ten years later. J Bone Joint Surg Am 88: 1117-1132, 2006.
3. Tan G, Kang PD and Pei FX: Glucocorticoids affect the metabolism of bone marrow stromal cells and lead to osteonecrosis of the femoral head: A review. Chin Med J 125: 134-139, 2012.
4. Tait AS, Butts CL and Sternberg EM: The role of glucocorticoids and progestins in inflammatory, autoimmune, and infectious disease. J Leukoc Biol 84: 924-931, 2008.
5. Kirwan JR: The effect of glucocorticoids on joint destruction in rheumatoid arthritis. The arthritis and rheumatism council Low-dose glucocorticoid study group. N Engl J Med 333: 142-146, 1995.
6. Salmon SE, Crowley JJ, Grogan TM, Finley P, Pugh RP and Barlogie B: Combination chemotherapy, glucocorticoids, and interferon alfa in the treatment of multiple myeloma: A Southwest oncology group study. J Clin Oncol 12: 2405-2414, 1994.
7. Hall ED and Braughler JM: Glucocorticoid mechanisms in acute spinal cord injury: A review and therapeutic rationale. Surg Neurol 18: 320-327, 1982.
8. Mont MA, Zywiel MG, Marker DR, McGrath MS and Delanois RE: The natural history of untreated asymptomatic osteonecrosis of the femoral head: A systematic literature review. J Bone Joint Surg Am 92: 2165-2170, 2010.
9. Boss JH: Experimental models of osteonecrosis of the femoral head. J Orthop Sci 9: 533-534, 2004.
10. Lavernia CJ, Sierra RJ and Grieco FR: Osteonecrosis of the femoral head. J Am Acad Orthop Surg 7: 250-261, 1999.
11. Kerachian MA, Cournoyer D, Harvey EJ, Chow TY, Bégin LR, Nahal A and Séguin C: New insights into the pathogenesis of glucocorticoid-induced avascular necrosis: Microarray analysis of gene expression in a rat model. Arthritis Res Ther 12: R124, 2010.
12. Cenni E, Fotia C, Rustemi E, Yuasa K, Caltavuturo G, Giunti A and Baldini N: Idiopathic and secondary osteonecrosis of the femoral head show different thrombophilic changes and normal or higher levels of platelet growth factors. Acta Orthop 82: 42-49, 2011.
13. Hernigou P, Beaujean F and Lambotte JC: Decrease in the mesenchymal stem-cell pool in the proximal femur in corticosteroid-induced osteonecrosis. J Bone Joint Surg Br 81: 349-355, 1999.
14. Hernigou P and Beaujean F: Abnormalities in the bone marrow of the iliac crest in patients who have osteonecrosis secondary to corticosteroid therapy or alcohol abuse. J Bone Joint Surg Am 79: 1047-1053, 1997.
15. Jia Y, Chu TW and Zhou Y: Repair process in experimentally induced avascular necrosis of femoral head in rabbits. Chongqing Med, 2006.
16. Takaoka K, Yoshioka T, Hosoya T, Ono K and Takase T: The repair process in experimentally induced avascular necrosis of the femoral head in dogs. Arch Orthop Trauma Surg 99: 109-115, 1981.
17. Malizos KN, Quarles LD, Seaber AV, Rizk WS and Urbaniak JR: An experimental canine model of osteonecrosis: Characterization of the repair process. J Orthop Res 11: 350-357, 1993.
18. Shapiro F, Connolly S, Zurakowski D, Menezes N, Olear E, Jimenez M, Flynn E and Jaramillo D: Femoral head deformation and repair following induction of ischemic necrosis. J Bone Joint Surg Am 91: 2903-2914, 2009.
19. Koromila T, Baniwal SK, Song YS, Martin A, Xiong J and Frenkel B: Glucocorticoids antagonize RUNX2 during osteoblast differentiation in cultures of ST2 pluripotent mesenchymal cells. J Cell Biochem 115: 27-33, 2014.
20. O'Brien CA, Jia D, Plotkin LI, Bellido T, Powers CC, Stewart SA, Manolagas SC and Weinstein RS: Glucocorticoids act directly on osteoblasts and osteocytes to induce their apoptosis and reduce bone formation and strength. Endocrinology 145: 1835-1841, 2004.
21. Lee JS, Lee JS, Roh HL, Kim CH, Jung JS and Suh KT: Alterations in the differentiation ability of mesenchymal stem cells in patients with nontraumatic osteonecrosis of the femoral head: Comparative analysis according to the risk factor. J Orthop Res 24: 604-609, 2006.

22. Houdek MT, Wyles CC, Packard BD, Terzic A, Behfar A and Sierra RJ: Decreased osteogenic activity of mesenchymal stem cells in patients with corticosteroid-induced osteonecrosis of the femoral head. J Arthroplasty 31: 893-898, 2016.
23. Wang BL, Sun W, Shi ZC, Lou JN, Zhang NF, Shi SH, Guo WS, Cheng LM, Ye LY, Zhang WJ and Li ZR: Decreased proliferation of mesenchymal stem cells in corticosteroid-induced osteonecrosis of femoral head. Orthopedics 31: 444, 2008.
24. Zhou DA, Zheng HX, Wang CW, Shi D and Li JJ: Influence of glucocorticoids on the osteogenic differentiation of rat bone marrow-derived mesenchymal stem cells. BMC Musculoskeletal Disord 15: 239, 2014.
25. Zhang W, Yang N and Shi XM: Regulation of mesenchymal stem cell osteogenic differentiation by glucocorticoid-induced leucine zipper (GILZ). J Biol Chem 283: 4723-4729, 2008.
26. Waterhouse E: Intravenous valproate for pediatric status epilepticus. Epilepsy Curr 3: 208-209, 2003.
27. Göttlicher M, Minucci S, Zhu P, Krämer OH, Schimpf A, Giavara S, Sleeman JP, Lo Coco F, Nervi C, Pelicci PG and Heinzel T: Valproic acid defines a novel class of HDAC inhibitors inducing differentiation of transformed cells. EMBO J 20: 6969-6978, 2001.
28. Cho HH, Park HT, Kim YJ, Bae YC, Suh KT and Jung JS: Induction of osteogenic differentiation of human mesenchymal stem cells by histone deacetylase inhibitors. J Cell Biochem 96: 533-542, 2005.
29. de Ruijter AJ, van Gennip AH, Caron HN, Kemp S and van Kuilenburg AB: Histone deacetylases (HDACs): Characterization of the classical HDAC family. Biochem J 370: 737-749, 2003.
30. Delcuve GP, Rastegar M and Davie JR: Epigenetic control. J Cell Physiol 219: 243-250, 2009.
31. Zheng QF, Wang HM, Wang ZF, Liu JY, Zhang Q, Zhang L, Lu YH, You H and Jin GH: Reprogramming of histone methylation controls the differentiation of monocytes into macrophages. FEBS J 284: 1309-1323, 2017.
32. Qin H, Zhao A, Zhang C and Fu X: Epigenetic control of reprogramming and transdifferentiation by histone modifications. Stem Cell Rev 12: 708-720, 2016.
33. Sepulveda H, Aguilar R, Prieto CP, Bustos F, Aedo S, Lattus J, van Zundert B, Palma V and Montecino M: Epigenetic signatures at the RUNX2-P1 and Sp7 gene promoters control osteogenic lineage commitment of umbilical Cord-derived mesenchymal stem cells. J Cell Physiol 232: 2519-2527, 2017.
34. Shahbazian MD and Grunstein M: Functions of site-specific histone acetylation and deacetylation. Annu Rev Biochem 76: 75-100, 2007.
35. Hatakeyama Y, Hatakeyama J, Takahashi A, Oka K, Tsuruga E, Inai T and Sawa Y: The effect of valproic Acid on mesenchymal pluripotent cell proliferation and differentiation in extracellular matrices. Drug Target Insights 5: 1-9, 2011.
36. Paino F, La Noce M, Tirino V, Naddeo P, Desiderio V, Pirozzi G, De Rosa A, Laino L, Altucci L and Papaccio G: Histone deacetylase inhibition with valproic acid downregulates osteocalcin gene expression in human dental pulp stem cells and osteoblasts: Evidence for HDAC2 involvement. Stem Cells 32: 279-289, 2014.
37. Xu Y, Hammerick KE, James AW, Carre AL, Leucht P, Giaccia AJ and Longaker MT: Inhibition of histone deacetylase activity in reduced oxygen environment enhances the osteogenesis of mouse adipose-derived stromal cells. Tissue Eng Part A 15: 3697-3707, 2009.
38. Lee S, Park JR, Seo MS, Roh KH, Park SB, Hwang JW, Sun B, Seo K, Lee YS, Kang SK, *et al*: Histone deacetylase inhibitors decrease proliferation potential and multilineage differentiation capability of human mesenchymal stem cells. Cell Prolif 42: 711-720, 2009.
39. Rashid MM, Akiba Y, Akiba N, Kaku M and Uoshima K: Effect of valproic acid on bone healing in rat. IADR/AADR/CADR General Session and Exhibition, 2013.
40. Grose AW, Gardner MJ, Sussmann PS, Helfet DL and Lorich DG: The surgical anatomy of the blood supply to the femoral head: Description of the anastomosis between the medial femoral circumflex and inferior gluteal arteries at the hip. J Bone Joint Surg Br 90: 1298-1303, 2008.
41. Zlotorowicz M and Czubak J: Vascular anatomy and blood supply to the femoral head. Osteonecrosis: 19-25, 2014.
42. Li GY, Feng Y, Cheng TS, Yin JM and Zhang CQ: Edaravone, a novel free radical scavenger, prevents steroid-induced osteonecrosis in rabbits. Rheumatology 52: 438-447, 2013.
43. Chen CH and Wang GJ: Alendronate in the prevention of collapse of the femoral head in nontraumatic osteonecrosis. Osteonecrosis 7: 265-271, 2014.
44. Nishida K, Yamamoto T, Motomura G, Jingushi S and Iwamoto Y: Pitavastatin may reduce risk of steroid-induced osteonecrosis in rabbits: A preliminary histological study. Clin Orthop Relat Res 466: 1054-1058, 2008.
45. Zhou D, Qi C, Chen YX, Zhu YJ, Sun TW, Chen F and Zhang CQ: Comparative study of porous hydroxyapatite/chitosan and whitlockite/chitosan scaffolds for bone regeneration in calvarial defects. Int J Nanomedicine 12: 2673-2687, 2017.
46. Luo S, Yang Y, Chen J, Zhong Z, Huang H, Zhang J and Cui L: Tanshinol stimulates bone formation and attenuates dexamethasone-induced inhibition of osteogenesis in larval zebrafish. J Orthopaedic Translation 4: 35-45, 2015.
47. Fujita T, Fukuyama R, Enomoto H and Komori T: Dexamethasone inhibits insulin-induced chondrogenesis of ATDC5 cells by preventing PI3K-Akt signaling and DNA binding of Runx2. J Cell Biochem 93: 374-83, 2004.
48. Livak KJ and Schmittgen TD: Analysis of relative gene expression data using real-time quantitative PCR and the $2^{-\Delta\Delta CT}$ method. Methods 25: 402-408, 2001.
49. Zhang YL, Yin JH, Ding H, Zhang W, Zhang CQ and Gao YS: Vitamin K_2 prevents glucocorticoid-induced osteonecrosis of the femoral head in rats. Int J Biol Sci 12: 347-358, 2016.
50. Guo SC, Tao SC, Yin WJ, Qi X, Sheng JG and Zhang CQ: Exosomes from human synovial-derived mesenchymal stem cells prevent glucocorticoid-induced osteonecrosis of the femoral head in the rat. Int J Biol Sci 12: 1262-1272, 2016.
51. Siéssere S, Semprini M, Lopes RA, Sala MA and Mattos MC: Morphological and morphometric alterations induced by valproic acid on rat fetuses' Meckel's cartilage, lingual musculature, and submandibular gland. Int J Morphol 22: 133-137, 2004.
52. Welbat JU, Chaisawang P, Chaijaroonkhanarak W, Prachaney P, Pannangrong W, Sripanidkulchai B and Wigmore P: Kaempferia parviflora extract ameliorates the cognitive impairments and the reduction in cell proliferation induced by valproic acid treatment in rats. Ann Anat 206: 7-13, 2016.
53. Cho HH, Park HT, Kim YJ, Bae YC, Suh KT and Jung JS: Induction of osteogenic differentiation of human mesenchymal stem cells by histone deacetylase inhibitors. J Cell Biochem 96: 533-542, 2005.
54. Jeon MJ, Kim JA, Kwon SH, Kim SW, Park KS, Park SW, Kim SY and Shin CS: Activation of peroxisome proliferator-activated receptor-gamma inhibits the Runx2-mediated transcription of osteocalcin in osteoblasts. J Biol Chem 278: 23270-23277, 2003.
55. Morimoto E, Li M, Khalid AB, Krum SA, Chimge NO and Frenkel B: Glucocorticoids Hijack Runx2 to stimulate *Wif1* for suppression of osteoblast growth and differentiation. J Cell Physiol 232: 145-153, 2017.
56. Shi XM, Chutkan N, Hamrick MW and Isales CM: Mechanism of glucocorticoid-induced osteoporosis: An update. Intech, 2012. DOI: 10.5772/53978.
57. Marquez-Curtis LA, Qiu Y, Xu A and Janowska-Wieczorek A: Migration, proliferation, and differentiation of cord blood mesenchymal stromal cells treated with histone deacetylase inhibitor valproic acid. Stem Cells Int 2014: 610495, 2014.
58. Tomé M, López-Romero P, Albo C, Sepúlveda JC, Fernández-Gutiérrez B, Dopazo A, Bernad A and González MA: miR-335 orchestrates cell proliferation, migration and differentiation in human mesenchymal stem cells. Cell Death Differ 18: 985-995, 2011.
59. Ciciarello M, Zini R, Rossi L, Salvestrini V, Ferrari D, Manfredini R and Lemoli RM: Extracellular purines promote the differentiation of human bone marrow-derived mesenchymal stem cells to the osteogenic and adipogenic lineages. Stem Cells Dev 22: 1097-1111, 2013.
60. Ding H, Wang T, Xu D, Cha B, Liu J and Li Y: Dexamethasone-induced apoptosis of osteocytic and osteoblastic cells is mediated by TAK1 activation. Biochem Biophys Res Commun 460: 157-163, 2015.
61. Kim SM, Kim YG, Park JW, Lee JM and Suh JY: The effects of dexamethasone on the apoptosis and osteogenic differentiation of human periodontal ligament cells. J Periodontal Implant Sci 43: 168-176, 2013.
62. Pang J, Huang H, Zhang Q, *et al*: The effect of dexamethasone on the proliferation and apoptosis of human bone marrow mesenchymal stem cells in vitro. Modern Med J China, 2008.

63. Gao B, Huang Q, Jie Q, Zhang HY, Wang L, Guo YS, Sun Z, Wei BY, Han YH, Liu J, *et al*: Ginsenoside-Rb2 inhibits dexamethasone-induced apoptosis through promotion of GPR120 induction in bone marrow-derived mesenchymal stem cells. Stem Cells Dev 24: 781-790, 2015.
64. Komori T: Regulation of osteoblast differentiation by Runx2. Adv Exp Med Biol 658: 43-49, 2010.
65. Rimando MG, Wu HH, Liu YA, Lee CW, Kuo SW, Lo YP, Tseng KF, Liu YS and Lee OK: Glucocorticoid receptor and Histone deacetylase 6 mediate the differential effect of dexamethasone during osteogenesis of mesenchymal stromal cells (MSCs). Sci Rep 6: 37371, 2016.
66. Pujols L, Mullol J, Pérez M, Roca-Ferrer J, Juan M, Xaubet A, Cidlowski JA and Picado C: Expression of the human glucocorticoid receptor alpha and beta isoforms in human respiratory epithelial cells and their regulation by dexamethasone. Am J Respir Cell Mol Biol 24: 49-57, 2001.
67. Li LB, Leung DY, Martin RJ and Goleva E: Inhibition of histone deacetylase 2 expression by elevated glucocorticoid receptor beta in steroid-resistant asthma. Am J Respir Crit Care Med 182: 877-883, 2010.
68. Adcock IM: Glucocorticoid-regulated transcription factors. Pulm Pharmacol Ther 14: 211-219, 2001.
69. Zhang YY, Li X, Qian SW, Guo L, Huang HY, He Q, Liu Y, Ma CG and Tang QQ: Down-regulation of type I Runx2 mediated by dexamethasone is required for 3T3-L1 adipogenesis. Mol Endocrinol 26: 798-808, 2012.
70. Adcock IM, Cosio B, Tsaprouni L, Barnes PJ and Ito K: Redox regulation of histone deacetylases and glucocorticoid-mediated inhibition of the inflammatory response. Antioxid Redox Signal 7: 144-152, 2005.
71. Ito K, Yamamura S, Essilfie-Quaye S, Cosio B, Ito M, Barnes PJ and Adcock IM: Histone deacetylase 2-mediated deacetylation of the glucocorticoid receptor enables NF-kappaB suppression. J Exp Med 203: 7-13, 2006.
72. Okazaki S, Nagoya S, Matsumoto H, Mizuo K, Sasaki M, Watanabe S, Yamashita T and Inoue H: Development of non-traumatic osteonecrosis of the femoral head requires toll-like receptor 7 and 9 stimulations and is boosted by repression on nuclear factor kappa B in rats. Lab Invest 95: 92-99, 2015.
73. Chen S, Li J, Peng H, Zhou J and Fang H: Administration of erythropoietin exerts protective effects against glucocorticoid-induced osteonecrosis of the femoral head in rats. Int J Mol Med 33: 840-848, 2014.
74. Han N, Yan ZQ, Guo CA, Shen F, Liu J, Shi YX and Zhang ZY: Effect of rifampicin on the risk of steroid-induced osteonecrosis of the femoral head. Orthop Surg 2: 124-133, 2010.
75. Tseng MT, Hsieh SC, Shun CT, Lee KL, Pan CL, Lin WM, Lin YH, Yu CL and Hsieh ST: Skin denervation and cutaneous vasculitis in systemic lupus erythematosus. Brain 129: 977-985, 2006.
76. Suda S, Katsura K, Kanamaru T, Saito M and Katayama Y: Valproic acid attenuates ischemia-reperfusion injury in the rat brain through inhibition of oxidative stress and inflammation. Eur J Pharmacol 707: 26-31, 2013.
77. Rao T, Wu F, Xing D, Peng Z, Ren D, Feng W, Chen Y, Zhao Z, Wang H, Wang J, *et al*: Effects of valproic Acid on axonal regeneration and recovery of motor function after peripheral nerve injury in the rat. Arch Bone Jt Surg 2: 17-24, 2014.
78. Zhang Z, Qin X, Tong N, Zhao X, Gong Y, Shi Y and Wu X: Valproic acid-mediated neuroprotection in retinal ischemia injury via histone deacetylase inhibition and transcriptional activation. Exp Eye Res 94: 98-108, 2012.
79. Hwabejire JO, Lu J, Liu B, Li Y, Halaweish I and Alam HB: Valproic acid for the treatment of hemorrhagic shock: A dose-optimization study. J Surg Res 186: 363-370, 2014.
80. Krishnamoorthy G, Karande S, Ahire N, Mathew L and Kulkarni M: Bone metabolism alteration on antiepileptic drug therapy. Indian J Pediatr 76: 377-383, 2009.
81. Lee HS, Lee CS, Jang JS, Lee JD and Um SM: Changes of serum alkaline phosphatase and osteocalcin during fracture healing. J Korean Orthopaedic Association 37: 411-415, 2002.
82. Komnenou A, Karayannopoulou M, Polizopoulou ZS, Constantinidis TC and Dessiris A: Correlation of serum alkaline phosphatase activity with the healing process of long bone fractures in dogs. Vet Clin Pathol 34: 35-38, 2005.
83. Floerkemeier T, Hirsch S, Budde S, Radtke K, Thorey F, Windhagen H and von Lewinski G: Bone turnover markers failed to predict the occurrence of osteonecrosis of the femoral head: A preliminary study. J Clin Lab Anal 26: 55-60, 2012.